Journal of Chromatographic Science 2012;50:324–334
doi:10.1093/chromsci/bms033

Article

Chemometrically Assisted Development and Validation of LC–UV and LC–MS Methods for Simultaneous Determination of Torasemide and its Impurities

Zarko Jovic[1], Ljiljana Zivanovic[2*], Marina Radisic[1], Ana Protic[2] and Marija Malesevic[1]

[1]Medicines and Medical Devices Agency of Serbia, National Control Laboratory, Vojvode Stepe 458, 11000 Belgrade, Serbia, and [2]University of Belgrade, Department of Drug Analysis, Faculty of Pharmacy, Vojvode Stepe 450, 11 152 Belgrade, Serbia

*Author to whom correspondence should be addressed. Email: ljzivan@pharmacy.bg.ac.rs

Received 18 February 2011; revised 8 June 2011

Complete evaluation of chromatographic behavior and establishment of optimal experimental conditions for determination of torasemide and its four impurities are determined by experimental design. Fractional factorial and 3^n full factorial design were employed for efficient and rapid optimization of liquid chromatography–ultraviolet and liquid chromatography–mass spectrometry (LC–MS) methods.

Separation is achieved on a Zorbax SB C_{18} analytical column (250 x 4.6 mm, 5 μm) with mobile phase consisting of acetonitrile and 10 mM ammonium formate (pH 2.5 with formic acid) in gradient mode. The flow rate is 1 mL min^{-1}, the temperature of the column is 25°C and UV detection is performed at 290 nm. The efficiency of ionization in electrospray ionization is higher than in atmospheric pressure chemical ionization mode; therefore, it is further used for analysis of torasemide and its impurities. Both methods meet all validation criteria. The calibration curves show high linearity with the coefficients of correlation (*r*) greater than 0.9982. The obtained recovery values (95.78–104.92%) and relative standard deviation values (0.12–5.56%) indicate good accuracy and precision. Lower limit of detection (LOD) and limit of quantitation (LOQ) values are obtained with the LC–MS method, indicating higher sensitivity of the proposed method.

Introduction

Torasemide (Figure 1A) is a loop diuretic. Its chemical structure, 1-isopropyl-3-(4-*m*-toluidinopyridine-3-sulphonyl) urea, is not related to other loop diuretics, such as furosemide, although their mechanisms of actions are similar (1, 2). Torasemide acts in the ascending limb of the Henle loop by inhibiting tubular reapsorption of sodium and chloride and interacting with the sodium/chloride/potassium/ co-transport system (3, 4). It has been considered suitable for a broad spectrum of clinical settings, including heart failure, hepatic cirrhosis, hypertension and chronic renal failure (5).

Impurities present in the dosage forms might lead to problems associated with toxicity, bioavailability or different pharmaceutical products' performance. According to International Conference on Harmonization (ICH) guidelines on impurities in new drug products, identification and quantitation is necessary for all impurities above 0.1% level (6, 7). Therefore, the paramount of modern pharmaceutical analysis is determination of the active ingredients and their impurities to assure a high quality of products, without changes in chemical, pharmacological and toxicological properties. Impurities of torasemide that could occur in the drug product are 4-(3-methylphenylamino)-3-pyridinesulfonamide (R2, Figure 1B), *N*-(ethylaminocarbonyl)-4-(3-methylphenylamino)-3-pyridinesulfonamide (R3, Figure 1C), *N*-(butylaminocarbonyl)-4-(3-methylphenylamino)-3-pyridinesulfonamide (R6, Figure 1D) and 3,4-dihydro-4-(3-methylphenyl)-2H-pyrido[4,3-e]-1,2,4-thiadiazine-1,1-dioxide (R4, Figure 1E). Impurities R3 and R6 can be formed during synthesis by a parallel reaction between 4-(3-methylphenylamino)-3-pyridinesulfonamide and ethylisocyanate or butylisocyanate, and are synthetic impurities. Impurity R2 is both a potential degradation product and synthetic impurity, because during synthesis of torasemide it can be disintegrated to impurity R4 (8). The control specification for all listed impurities is up to a maximum of 0.3%.

During a literature survey, several methods for the analysis of torasemide and its metabolites in human plasma and urine have been found. These include high-performance liquid chromatography (HPLC) with ultraviolet (UV) (9, 10) or electrochemical detection (11), gas chromatographic–mass spectrometry(GC–MS) (12) and capillary zone electrophoresis with an experimental design approach (13). Also, liquid chromatography–mass spectrometry (LC–MS) (14–17) and capillary electrophoresis (18) methods were found for the determination of torasemide in a mixture of diuretics in urine.

However, to our knowledge, there is no work about the simultaneous determination of torasemide and its four impurities in pharmaceutical dosage forms. Therefore, the aim of this work was evaluation of the chromatographic behavior and development of sensitive, reliable LC–MS and LC–UV methods for determination of torasemide and its impurities in pharmaceutical dosage form. The complete chromatographic behavior and optimal chromatographic conditions were evaluated with the assistance of experimental design. In this way, maximum information was obtained with a limited number of experiments. Because impurities are usually present in small quantities, it was decided to develop the LC–MS method. This technique couples high resolution chromatographic separation with sensitive and specific mass spectrometric detection, which is clearly advantageous, particularly because many compounds with similar or identical retention characteristics have quite different mass spectra and can therefore be differentiated. (19). In this way, the MS detection could reveal the presence of potentially unknown impurities in dosage form. The presented method is planned to be used in further forced degradation studies. Two ionization modes, electrospray ionization (ESI) and atmospheric pressure chemical ionization (APCI) for LC–MS analysis of all five compounds were evaluated. HPLC

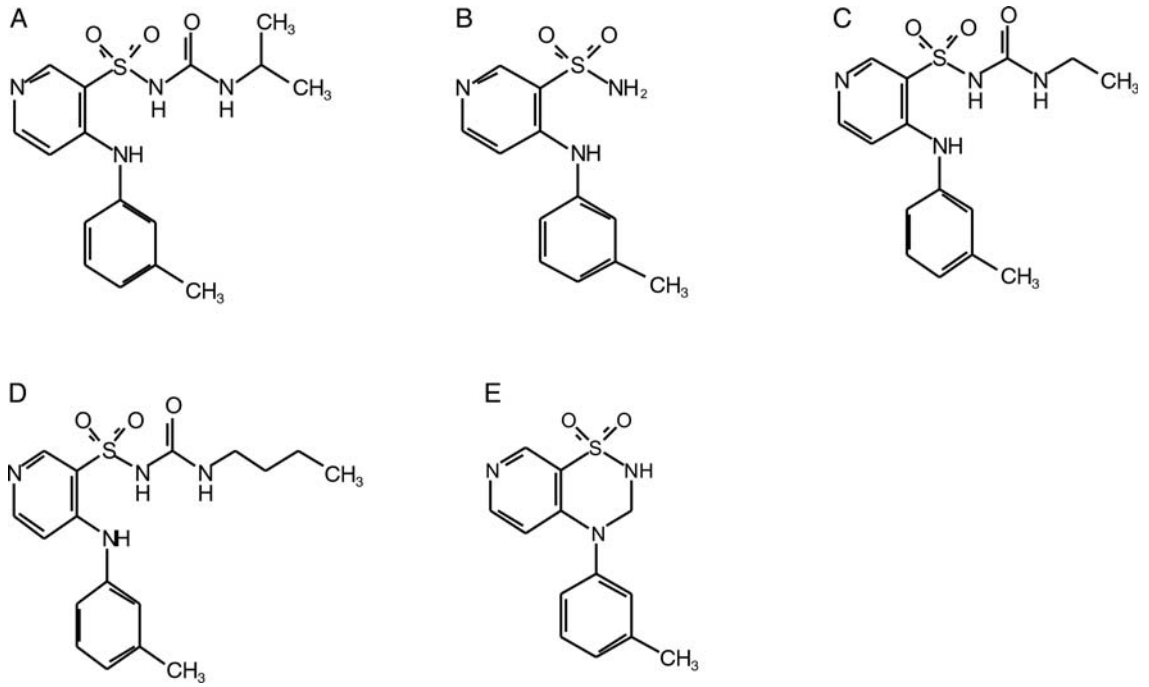

Figure 1. (A) Structure of torasemide; structures of impurities: (B) R2, (C) R3, (D) R6, (E) R4.

with UV detection is a widely used analytical technique in quality control of pharmaceuticals. For those reasons, simultaneous LC–MS and LC–UV methods have been developed.

Both analytical methods were successfully validated in accordance with ICH guidelines (20). The selectivity, limits of detection and quantification, linearity, accuracy and precision (repeatability) were determined and obtained results were compared. Subsequently, the applicability of the proposed methods on the tablet dosage form has been demonstrated.

Experimental

Chemicals and reagents

Standards of torasemide, impurities R2, R3, R4, R6 and Diuver tablets (containing 10 mg of torasemide) were obtained from Pliva (Zagreb, Croatia). All reagents were of analytical grade. Acetonitrile (Merck, Germany), ammonium formate (Fluka, Germany) and formic acid (Merck, Germany) were used to prepare the mobile phase. Water for chromatography was deionized using an Easy pure RF (Barnstead) purification system. The mobile phase was prepared daily, degassed and vacuum filtered before use through a Millipore 0.45 μm (47 mm diameter) nylon membrane filter (Millipore, Milford, MA). Millex syringe driven filter units of 0.45 μm (Millipore, Milford, MA) were used to filter the samples.

Equipment

The LC coupled mass spectrometer detector system Agilent 1100 series (Agilent Technologies, Germany) consisted of binary pump, degasser, thermostated autosampler, thermostated column compartment, diode-array detector and a single quadrupole mass analyzer (G1946D). Data collection and processing were performed using Agilent Chemstation software (Agilent Technologies, Germany). Design-ExpertSoftware version 7.0, Excel 2003 and Statistica 8 were used for statistical analysis.

Chromatographic conditions

The chromatographic separation was performed on a Zorbax SB C_{18} analytical column (250 x 4.6 mm, 5 μm, Agilent) with column temperature set at 25°C. The mobile phase was an aqueous solution of 10 mM ammonium formate, adjusted to pH 2.5 with formic acid (mobile phase A) and acetonitrile (mobile phase B), with gradient elution: 0 min, B 30%; 11.2 min, B 60%; 11.3 min, B 30 %, hold for 10 minutes. The flow rate was 1 mL min^{-1} and the injection volume was 30 μL for LC–UV analysis and 10 μL for LC–MS analysis. Detection was performed at 290 nm.

Mass spectrometric conditions

An ESI technique was used. All analytes were analyzed in positive ionization mode. Optimization of LC–MS conditions was carried out using flow injection analysis (FIA) of the analytes (10 μL of 10 μg mL^{-1} standard solutions for all substances). The optimized parameters of the interface were: drying gas (N_2) flow rate, 12.0 L min^{-1}; nebulizer gas pressure, 60 psig; temperature, 350°C; capillary voltage, 3000 V; gain, 2. To quantify torasemide and its impurities, selective ion monitoring (SIM) of protonated molecular ions $[M + H]^+$ at m/z: 349 (torasemide), 264 (impurity R2), 276 (impurity R4), 335 (impurity R3) and 363 (impurity R6) was used.

Standard solutions

Stock solution of torasemide was prepared by dissolving the standard substance in the acetonitrile–water (50:50, v/v) to

obtain a final concentration of 1 mg mL^{-1}. Stock solutions of each impurity were prepared by dissolving the standard substances of R2, R3, R4 and R6 in the acetonitrile–water (50:50, *v/v*) to obtain a final concentration of 0.1 mg mL^{-1}.

For linearity testing, seven standard solutions of torasemide and its impurities were prepared diluting stock solutions with acetonitrile–10 mM ammonium formate, pH 2.5 (50:50, *v/v*). For the LC–UV analysis, the concentration ranges for torasemide and its impurities were 70–130 and 0.1–10 μg mL^{-1}, respectively. For the LC–MS analysis, the concentration ranges were 0.7–1.3 μg mL^{-1} for torasemide and 0.01–1.0 μg mL^{-1} for impurities.

The investigation of accuracy and precision of the method was evaluated at three concentrations of torasemide and its impurities. For the LC–UV analysis, the concentration levels for torasemide and its impurities were 70, 100 and 130 μg mL^{-1} and 0.1, 1.0 and 10 μg mL^{-1}, respectively. For the LC–MS analysis, the concentration levels were 0.7, 1.0 and 1.3 μg mL^{-1} for torasemide and 0.01, 0.1 and 1.0 μg mL^{-1} for impurities. The solutions for investigation of accuracy of the method were prepared adding known amount of the analyte into the placebo mixture.

The limit of detection (LOD) and limit of quantitation (LOQ) were determined with solutions obtained by diluting the stock solution of each compound with acetonitrile–10 mM ammonium formate, pH 2.5 (50:50, *v/v*).

All solutions were protected from light due to light sensitivity of the investigated substances. Under the stated experimental conditions, during development and validation procedures, stability related problems were not noticed with the standard and sample solutions.

Preparation of sample solutions

An amount of powdered tablets that contained 10 mg of torasemide was transferred to a 50 mL volumetric flask and dissolved in approximately 35 mL of acetonitrile–water (50:50, *v/v*) with the assistance of an ultrasonic bath for 15 min. The solution was then diluted to volume with the same solvent and filtered through a 0.45 μm filter. For the LC–UV analysis, the filtered solution was diluted with acetonitrile–10 mM ammonium formate, pH 2.5 (50:50, *v/v*) to produce the expected torasemide concentration of 0.1 mg mL^{-1}. For the LC–MS analysis, solution with torasemide concentration of 0.1 mg mL^{-1} was further diluted with acetonitrile–10 mM ammonium formate, pH 2.5 (50:50, *v/v*) to obtain torasemide concentrations of 0.01 and 0.001 mg mL^{-1} for related substances and assay tests, respectively. All solutions were freshly prepared before analysis and kept protected from light.

Results and Discussion

Optimization of chromatographic conditions

In separation science, development of a method involves determination of the optimal experimental conditions that enable sufficient resolution of the relevant peaks and furnish adequate and robust assay results in an acceptable analysis time (21). The HPLC is primarily based on partition separation mechanism of the analytes between the mobile and stationary phases, which mostly depends on the properties of the analytes, pH and composition of the mobile phase and type of stationary phase (22). Therefore, based on the nature of the investigated substances, the stationary phase was chosen and further optimal chromatographic conditions were determined with the assistance of fractional factorial 2^{4-1} and 3^n full factorial design.

Torasemide and its four impurities have very similar physical-chemical properties. The log*P* values are 1.97, 1.31, 1.55, 2.52 and 1.70 for torasemide, R2, R3, R6 and R4, respectively. The C_{18} packing columns were shown to be the most suitable according to the lipophilic nature of the compounds. Initially, four columns were examined (Zorbax Extend C_{18}, Xterra RP_{18}, Chromolith RP_{18} and Zorbax SB C_{18}) and it was decided to continue the investigation on Zorbax SB C_{18}. This decision was based on the properties of this column, which is packed with specific, spherical microparticles, allowing high efficiency of separation, compatibility with the high-sensitivity detectors and typical volatile mobile phase additives used for LC–MS. Use of this column enabled tight, symmetrical peaks with good separation of all analyzed compounds.

Among organic modifiers used in reversed phase (RP)–HPLC, it was decided to use acetonitrile based on better peak symmetries and shorter analysis run time. The addition of buffer was inevitable, and buffers suitable for LC–MS analysis were examined (ammonium formate, ammonium acetate and trifluoroacetic acid). Concentrations of these buffers were varied in the range from 5–10 mM. The best combination of ionization efficiency and chromatographic peak shape was found with the 10 mM ammonium formate; higher concentrations of the buffer were not investigated because they are not recommended when an MS detector is used.

All compounds are ampholyts with two *pKa* values. The first *pKa* is the same for all substances and arose from basic properties of the compounds ($pKa1_{torasemide,\ R2,\ R3,\ R4,\ R6} = 4.20$). The second *pKa* arose from acidic properties and differs among compounds ($pKa2_{\text{torasemide, R3, R6}} = 5.92$, $pKa2_{R2} = 9.62$, $pKa2_{R4} = 9.46$). Therefore, it was expected that the pH

Table I
Investigated Variables and their Levels Studied in the FFD 2^{4-1} and 3^2 Full Factorial Designs

Variables	Investigated levels		
	−1	0	+1
(x_1) Acetonitrile (%)	20	/	60
(x_2) pH value of the water phase	2.0	2.5	3.0
(x_3) Temperature of the column	15	25	35
(x_4) Strength of the buffer (mM)	0	/	10

Table II
Plan of the Experiments for the FFD 2^{4-1} Design for Four Variables and Corresponding Retention Factors for Torasemide and its Impurities

Exp. no.	Variables				Retention factors				
	x_1	x_2	x_3	x_4	R2	R4	R3	Torasemide	R6
1	−1	−1	−1	−1	2.70	3.18	9.43	18.11	36.64
2	+1	−1	−1	+1	0.18	0.25	0.25	0.37	0.66
3	−1	+1	−1	+1	3.56	4.71	7.21	14.46	34.89
4	+1	+1	−1	−1	0.21	0.21	0.21	0.21	0.44
5	−1	−1	+1	+1	2.34	2.66	8.57	16.68	30.19
6	+1	−1	+1	−1	0.09	0.13	0.17	0.23	0.44
7	−1	+1	+1	−1	1.91	2.70	5.00	9.43	25.89
8	+1	+1	+1	+1	0.19	0.39	0.10	0.19	0.35

of the water phase would have a significant influence on the retention behavior of the investigated ampholytes. This assumption was confirmed during preliminary experiments and it was decided to vary the pH of the water phase from 2–3. A pH above 3 was not investigated because molecules of torasemide and its impurities exist in molecular and ionic shapes.

The influence of the temperature of the column was investigated in the range from 15–35°C. These are commonly used temperatures in HPLC methods.

The fractional factorial design (FFD) was used to detect all variables that significantly influenced the chromatographic procedure. The aim of the screening phase is to decrease the number of experiments by determination of variables that have statistically significant influence on the chromatographic system (23). The number of experiments in FFD is given as $2^{k-p} + C$, where k is the number of variables, C is the number of replicates at the central point and p is a whole number that indicates how fractionated the experimental design is. When p is zero, the experimental design is full (24). The 2^{4-1} FFD resulting from eight experiments was conducted and the retention factors were the observed responses (25). The investigated variables and their domains are presented in Table I. High and

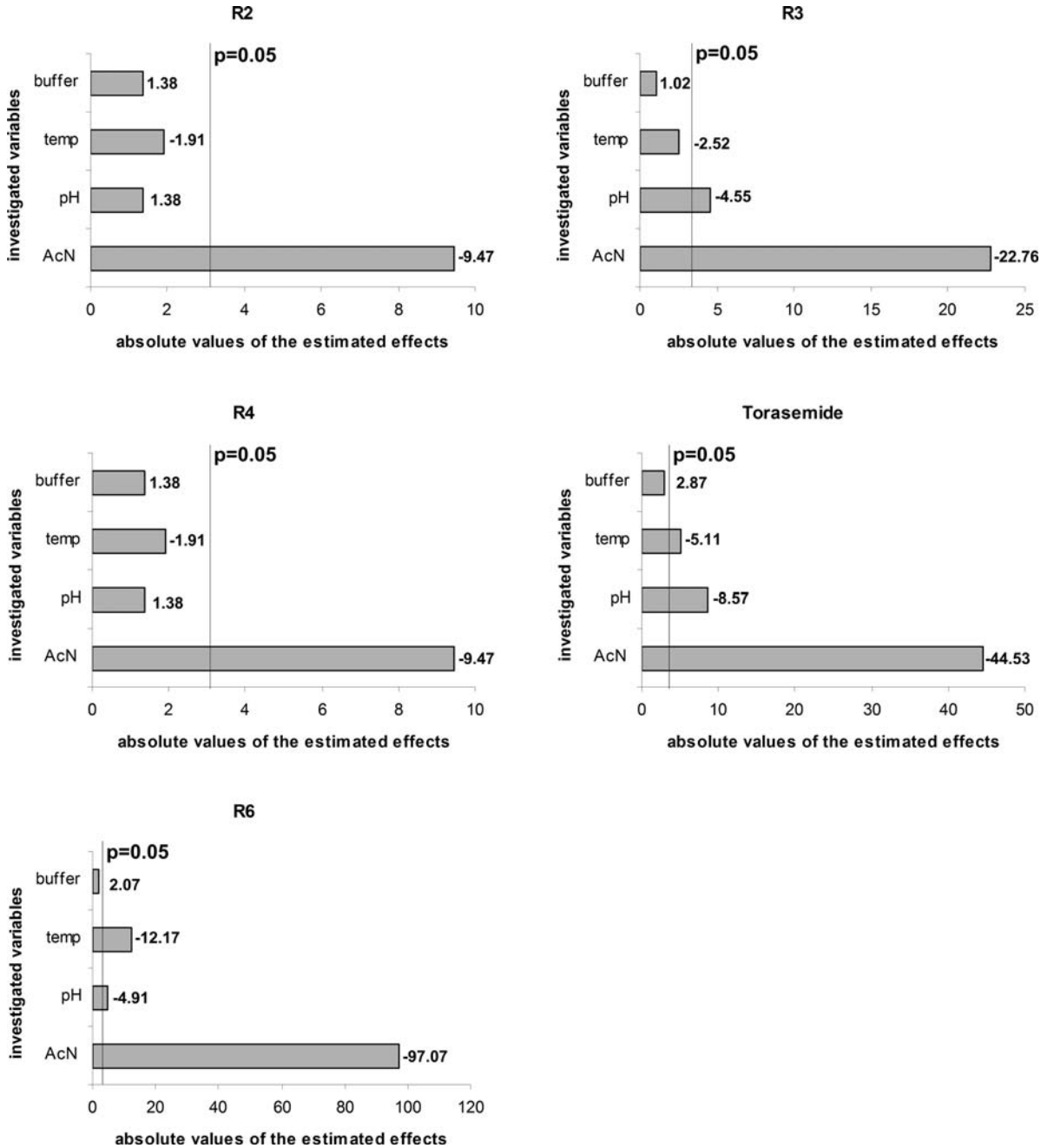

Figure 2. Representative Pareto charts of standardized effects (absolute value) obtained from the FFD show the influence of studied variables on the retention factors of R2, R3, R4, torasemide and R6.

low levels of each variable were defined during preliminary experiments and are denoted as +1 and −1. The observed response during FFD was the retention factor of all analyzed substances. The experimental plan of FFD and obtained retention factors are reported in Table II. All experiments were performed randomly and without repetition, except four experiments at the central point that enabled estimation of the statistical importance of the variables.

According to the obtained retention factors, the estimated effects and standardized effects were calculated. Critical *t*-value for $\alpha = 0.05$ and 3 degrees of freedom (DF) was 3.182 for all substances. All factors whose absolute values of the standardized effects are above critical *t*-value are statistically significant and those below this value are statistically insignificant. Pareto charts, of which the length of the bars is proportional to the absolute value of the standardized effects, are presented in Figure 2. The dashed line represents critical *t*-value and the importance of the presented variables can easily be observed.

In further work, statistically significant variables, percentage of acetonitrile, pH of the water phase and temperature of the column were thoroughly studied by employing optimization design. Similar structures and therefore similar chromatographic behavior of all five compounds caused difficulties in definition of the range of organic modifier. No range of acetonitrile could simultaneously satisfy acceptable separation and appropriate analysis run time. Therefore, it was necessary to establish a gradient elution. The developed gradient mode was reported in detail in a previous section. Two remaining variables were evaluated employing three-level full-factorial design. The previously mentioned design contains all possible combinations between the n variables on 3 levels, requiring $N = 3^n$ experiments (21). The experimental domain and plan of experiment are presented in Tables I and III, respectively. Controllable factors were held constant at defined levels (10 mM ammonium formate buffer according to better peak symmetries and gradient elution) and all experiments were performed randomly. Two responses were examined: retention factors for torasemide and its impurities and resolution between critical pair (impurities R2 and R4). The obtained responses for every experiment are presented in Table III. According to the results of experiments, the following response surface models were computed:

$$y = 0.94 + 0.23x_1 - 0.087x_2 - 0.0025x_1x_2 + 0.13x_1^2 + 0.0067x_2^2,$$

where y represents the retention factor of impurity R2,

$$y = 1.16 + 0.26x_1 - 0.085x_2 + 0.017x_1x_2 + 0.057x_1^2 + 0.0017x_2^2,$$

where y represents the retention factor of impurity R4,

$$y = 1.53 + 0.12x_1 - 0.092x_2 + 0.01x_1x_2 + 0.18x_1^2 + 0.0017x_2^2,$$

where y represents the retention factor of impurity R3,

$$y = 2.09 - 0.04x_1 - 0.093x_2 + 0.03x_1x_2 - 0.003x_1^2 - 0.003x_2^2,$$

Table III
Plan of Experiments in 3^n Full Factorial Designs for Torasemide, R2, R3, R4 and R6

Exp. no.	Variables		Retention factors					Resolution
	x_2	x_3	R2	R4	R3	Torasemide	R6	R2/R4
1	−1	−1	0.93	1.06	1.69	2.24	3.20	1.87
2	−1	+1	0.76	0.86	1.48	2.00	2.88	1.71
3	−1	0	0.84	0.95	1.58	2.12	3.04	1.79
4	+1	−1	1.39	1.54	1.91	2.10	2.95	2.22
5	+1	+1	1.21	1.41	1.74	1.98	2.78	3.36
6	+1	0	1.29	1.48	1.82	2.04	2.86	2.88
7	0	−1	1.03	1.25	1.61	2.18	3.09	3.28
8	0	+1	0.86	1.07	1.44	1.98	2.82	3.49
9*	0	0	0.94	1.16	1.53	2.09	2.96	3.49

*Four replicates at the center point

where y represents the retention factor of torasemide,

$$y = 2.96 - 0.08x_1 - 0.13x_2 + 0.037x_1x_2 - 0.005x_1^2,$$

where y represents the retention factor of impurity R6,

$$y = 3.41 + 0.52 \times_1 + 0.2 \times_2 + 0.32 \times_1 x_2 - 1.08 \times_1^2 - 0.035 \times_2^2,$$

where y represents the resolution between impurities R2 and R4.

The x_1 represents the pH of the mobile phase and x_2 represents the column temperature.

The 3D response surface graphs were obtained when system response was plotted against two quantitative variables (26). The 3D graphs for each of the evaluated responses are presented in Figure 3. Impurities R2 and R4 have the most similar chromatographic behavior; therefore, problems due to separation were expected. Similar chromatographic behavior was observed for torasemide and impurity R6, but regarding retention parameters, they are not close enough to disable the separation. To choose optimal chromatographic conditions, the resolution between the critical pair of impurities R2 and R4 was also evaluated. As concluded from the 3D graph, optimal separation could be achieved with a temperature of 25°C and pH of the water phase of 2.5. With these chromatographic conditions, satisfactory separation and acceptable analysis time were achieved.

Summarizing all the facts, it was clear that optimal chromatographic conditions included a mobile phase consisting of acetonitrile–10 mM ammonium formate buffer with pH adjusted to 2.5 in gradient mode. Column temperature was set at 25°C, flow rate was 1 mL min^{-1} and detection was performed at 290 nm. Under these conditions, retention factors (k) and peak symmetry (A_s) for all compounds, in addition to resolution (R_s) between peaks, were satisfied and fulfilled all requirements of system suitability testing (27). The values of system suitability parameters are presented in Table IV.

Optimization of MS conditions

Two ionization modes, ESI and APCI, for LC–MS analysis of torasemide and its impurities were evaluated.

According to the literature for torasemide (16, 28–30), both positive and negative modes for ESI and APCI could be applied. Because the production of positive ions is favored at acidic pH

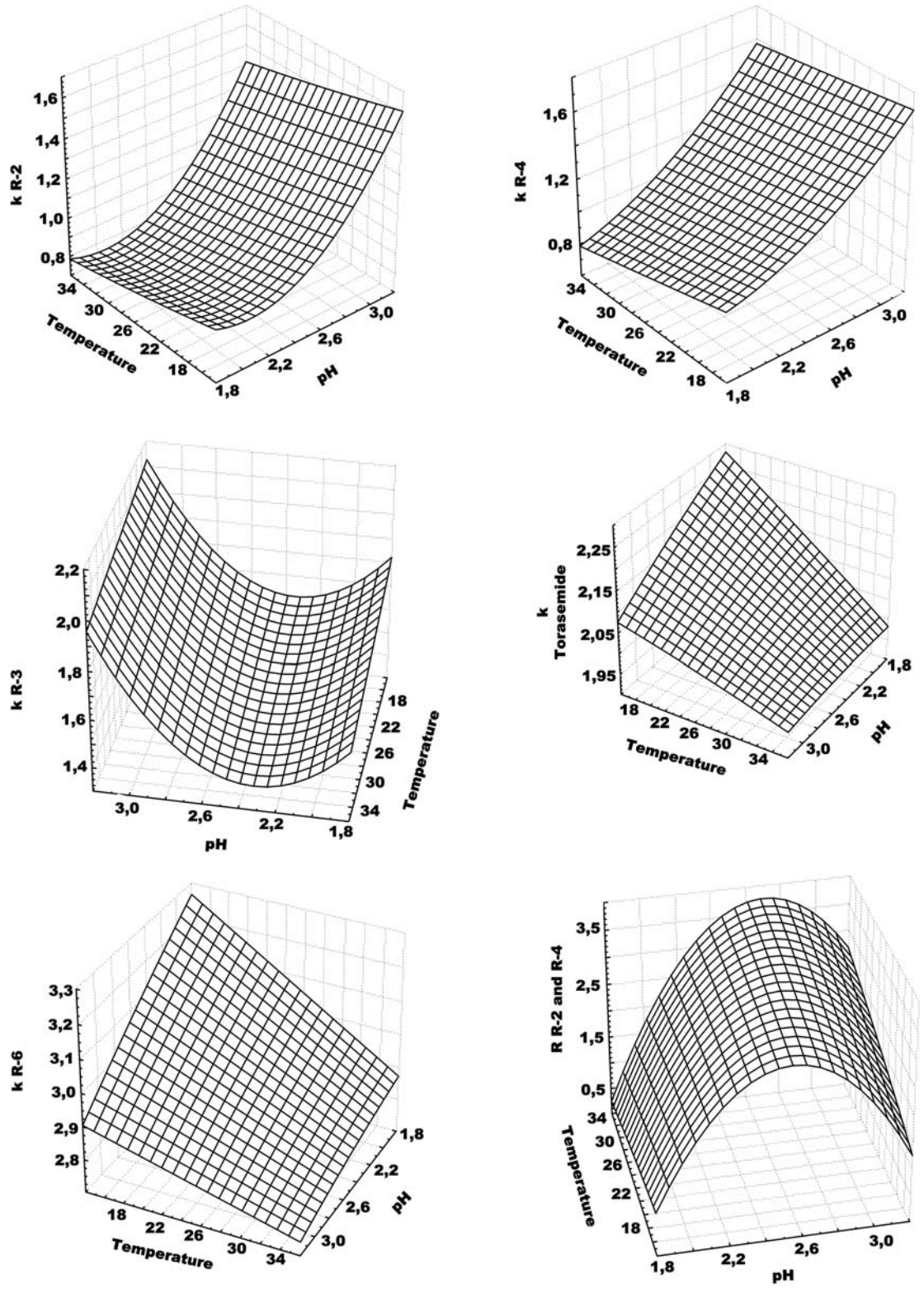

Figure 3. 3D graphs of the response surface for retention parameters of R2, R4, R3, torasemide and R6, and resolution factor for impurities R2 and R4 as a function of column temperature and pH.

(optimal chromatographic conditions), the positive mode was chosen. Positive ion mode, with a mobile phase consisting of ammonium formate–formic acid buffer and acetonitrile, involves the creation of $[M + H]^+$ ions and the possible presence of solvent adduct ions such as $[M + NH_4]^+$, $[M + H + ACN]^+$ and $[M + NH_4 + ACN]^+$ (15). In this study, the solvent

Table IV
System Suitability Data

Compound	Retention time (t_r)	Retention factor (k)	Symmetry (A_s)	Resolution (R_s)
R2	4.937	0.94	0.98	
R4	5.448	1.16	0.98	3.49[a]
R3	6.142	1.53	0.98	4.84[b]
Torasemide	7.373	2.09	0.74	6.28[c]
R6	9.415	2.96	0.98	10.04[d]

[a]R2 and R4
[b]R4 and R3
[c]R3 and torasemide
[d] torasemide and R6

Table V
The Protonated Molecular Ion and Fragment Ions of Torasemide and its Impurities, ESI–MS with optimal Fragmentor Voltage

Compound	Molecular weight	Protonated molecular ion, m/z	Fragment ions, m/z	Fragmentor[a] (V)	Fragmentor[b] (V)
R2	263	264	183/168	120	240
R4	275	276	183	160	200
R3	334	335	290/264	70	160
Torasemide	348	349	290/264	70	170
R6	362	363	290/264	100	180

[a]Fragmentor voltage for protonated molecular ion
[b]Fragmentor voltage for fragment ions

adduct ions, having very low intensities, were also detected. FIA was performed to determine the presence of diagnostic ions for each compound and to optimize MS parameters: vaporizer temperature, corrona current, capillary voltage, nebulizer pressure, drying gas flow and drying gas temperature.

The vaporizer temperature was varied from 250 to 450°C in positive APCI. The maximum intensity of signals of protonated molecular ions was achieved at 450°C.

The corona current was varied from 2 to 10 μA and the optimal values for all compounds were found at 8 μA. The capillary voltage was varied between 2000 and 4000 V. A slight improvement of sensitivity was observed at 3000 V.

The drying gas flow rate was varied from 3 to 9 L min^{-1} and the optimum flow rate was found at 6 L min^{-1}. The nebulizer pressure was tested between 30 and 60 psig, with no significant influence on the response (set at 60 psig). Conversely, an increase of gas temperature positively affected on the response of compounds, and gas temperature at 350°C was set as optimal (varied between 200 and 350°C).

For ESI, the capillary voltage, nebulizer pressure and drying gas temperature were varied in the same range as for APCI and the following optimal values were found: capillary voltage, 3000 V; nebulizer pressure, 60 psig; drying gas temperature 350°C and drying gas flow was set at 12.0 L min^{-1} (high flow rate).

APCI and ESI in positive ion mode provided the formation of protonated molecular ions $[M + H]^+$ at m/z: 349 (torasemide); 264 (impurity R2); 276 (impurity R4); 335 (impurity R3); 363 (impurity R6) as well as the characteristic product (fragment) ions of the studied analytes. Fragmentation of torasemide and its impurities R4, R3 and R6, leads to formation of fragment ions amongst which the fragment ion with m/z ratio corresponding to m/z ratio of protonated molecular ion of impurity R2 was also observed. Moreover, torasemide and impurities R3 and R6 gave the same fragment ion at m/z 290, due to the chemical structure similarity of compounds. To establish a reliable method for the simultaneous determination of torasemide and its impurities, it was necessary to achieve an optimal chromatographic separation. That goal is accomplished and is presented in a previous section.

Generally, more fragments could be found under the optimal conditions in the APCI mode, useful for identification purposes (in ESI mode, impurity R4 showed poor fragmentation with only one fragment ion found at m/z 183). On the other hand, the efficiency of ionization in ESI was higher than APCI and therefore more appropriate for quantitative applications. Considering the advantages and disadvantages of both APCI and ESI methods, ESI in positive mode was used for further analysis of torasemide and its impurities (SIM mode for quantification purposes and mass spectral data as well as retention time of target compounds for peak identification).

Table V presents the protonated molecular ion and fragment ions of torasemide and impurities R2, R4, R3 and R6 in ESI mode, with optimal fragmentor voltage. Mass spectra in ESI mode are presented in Figure 4.

Method validation

After the optimization procedure, the validation was performed according to the validation protocols that comply with the international guidelines on method validation (20). The objective of validation of an analytical procedure is to demonstrate that it is suitable for its intended purpose. The selectivity, linearity, accuracy, precision (repeatability), LOD and LOQ were determined for both LC–UV and LC–MS methods.

The selectivity was investigated by observing potential interferences between torasemide and its impurities with tablet excipients. The placebo mixture showed no peaks at the retention times of the compounds analyzed. Therefore, both methods showed good selectivity. Representative UV chromatograms of placebo mixture (Figure 5A) and working standard mixture (Figure 5B) are shown in Figure 5.

The linearity of an analytical procedure is its ability to obtain test results that are directly proportional to the concentration (amount) of analyte in the sample. The linearity was examined in the concentration range of 70–130 μg mL^{-1} for torasemide and 0.1–10 μg mL^{-1} for impurities R2, R3, R4 and R6 by applying LC–UV. The concentrations range of torasemide was 0.7–1.3 μg mL^{-1} and 0.01–1.0 μg mL^{-1} for its impurities in LC–MS. The specified ranges for the assay (70–130 % of torasemide expected concentration) and determinations of impurities (0.1–10 % of torasemide declared content in the sample) were derived considering ICH guidelines (20, 7). Each of these solutions was injected three times. Linear relationships of peak areas against concentrations were obtained by using the least squares method. Data from regression analysis of each component are presented in Table VI. The high linearity over the entire concentration range was demonstrated with the coefficients of correlation (r) greater than 0.9982. Hence, it can be concluded that the linearity is satisfied for both LC–UV and LC–MS methods.

The closeness of the measured value to the true value is its accuracy, which was calculated as recovery value of the known

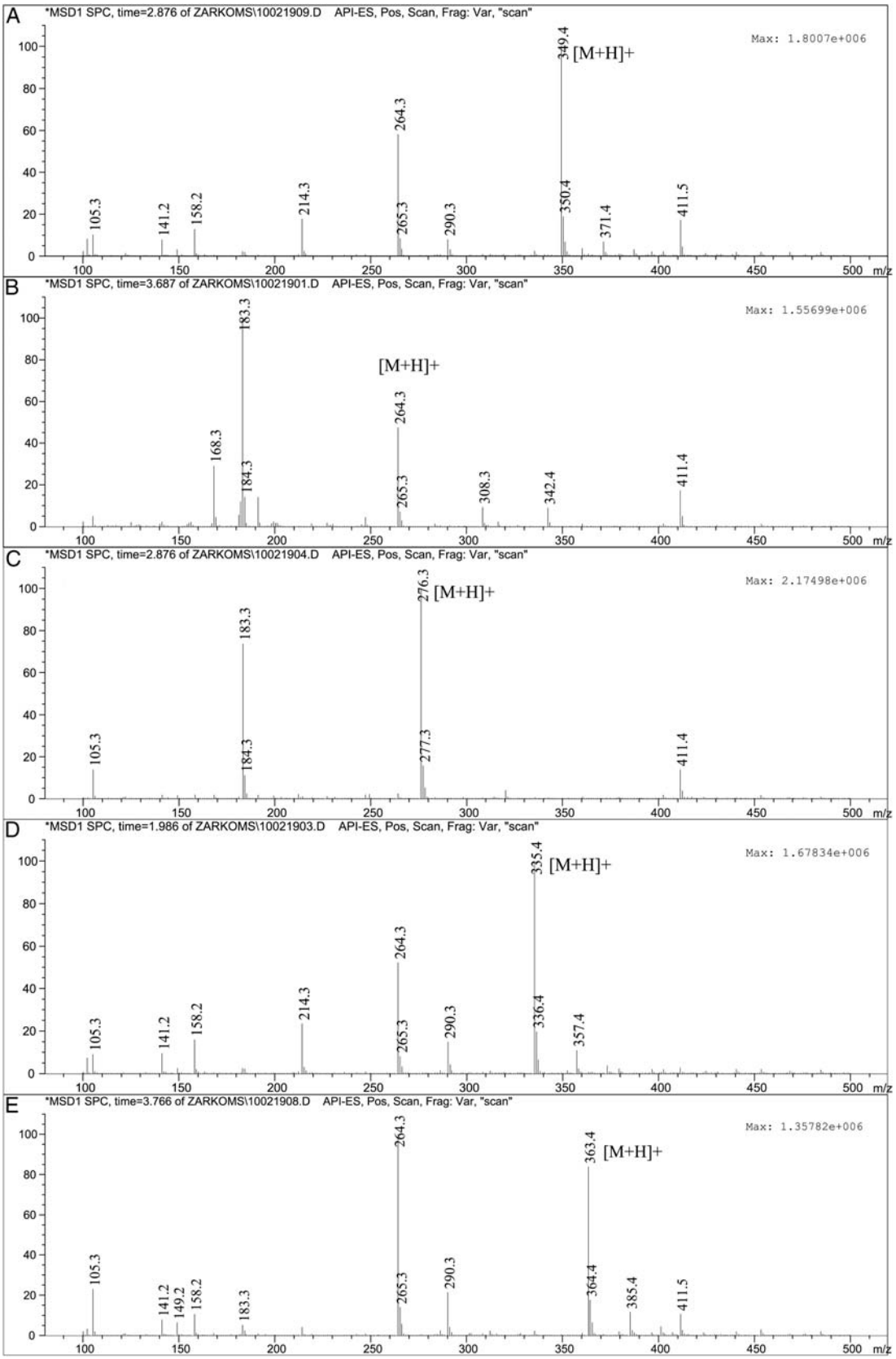

Figure 4. ESI–MS spectra of: (A) torasemide, (B) R2, (C) R4, (D) R3, (E) R6.

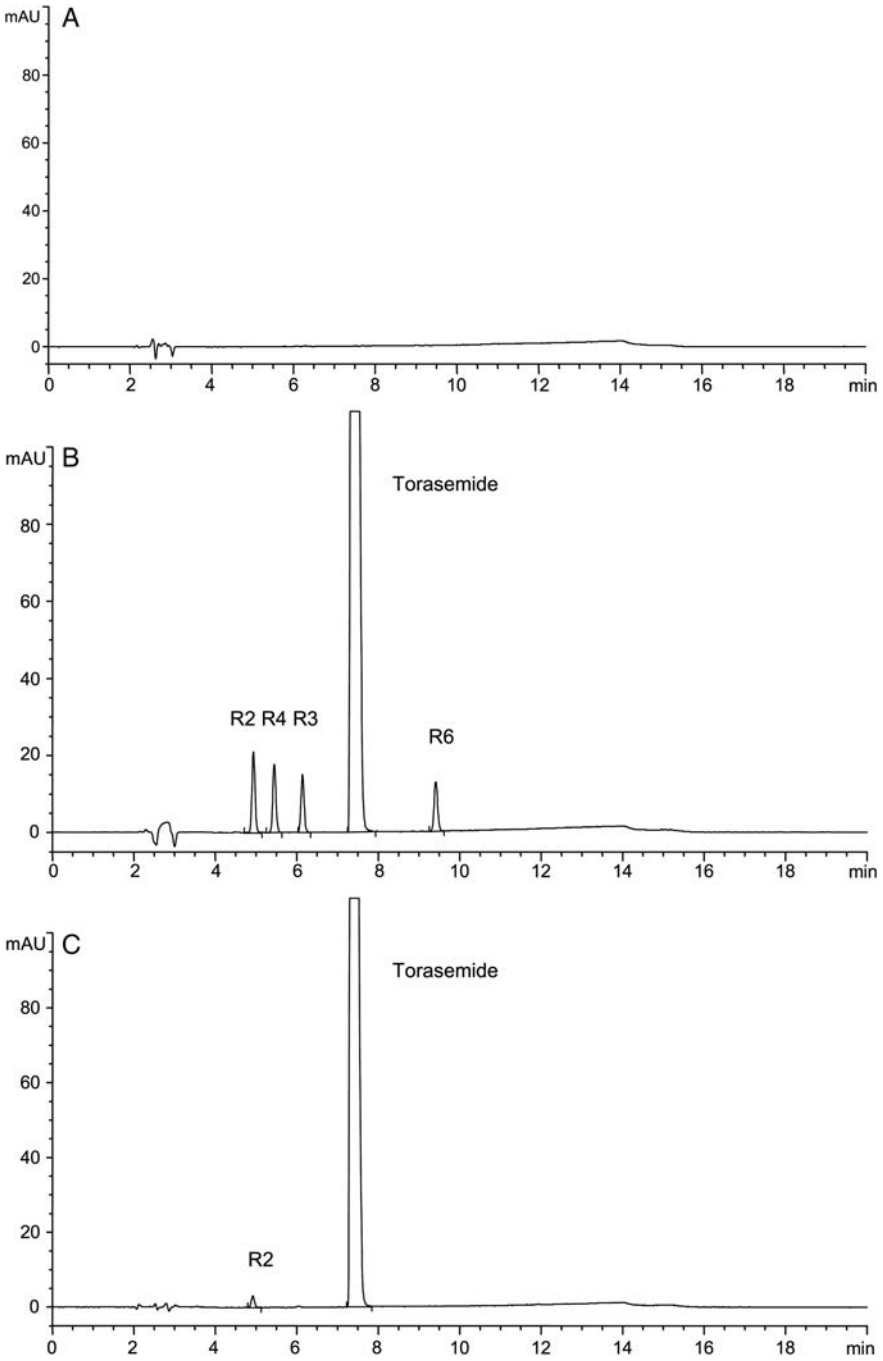

Figure 5. Representative UV chromatograms of: (A) placebo mixture, (B) working standard mixture, (C) sample solution of torasemide tablets.

Table VI
Regression Analysis Data, LOD and LOQ Values for LC–UV and LC–MS Methods

Compound	LC–UV				LC–MS			
	$y = ax + b$*	r	LOD μg mL^{-1}	LOQ μg mL^{-1}	$y = ax + b$*	r	LOD μg mL^{-1}	LOQ μg mL^{-1}
R2	90.281x + 4.577	0.9997	0.020	0.060	4E + 07x + 432007	0.9997	0.0003	0.0009
R4	84.479x + 2.117	0.9999	0.025	0.075	4E + 07x + 138278	0.9999	0.0002	0.0006
R3	65.636x + 4.582	0.9998	0.030	0.090	3E + 07x + 733744	0.9982	0.0004	0.0012
Torasemide	66.785x-145.6	0.9989	0.035	0.100	9E + 06x + 547684	0.9990	0.0002	0.0006
R6	59.995x + 5.552	0.9998	0.030	0.090	3E + 07x + 789633	0.9983	0.0002	0.0006

* $n = 7$

Table VII
Accuracy and Precision of the LC–UV and LC–MS Methods

Compound	LC–UV				LC–MS			
	Amount added ($\mu g\ mL^{-1}$)	Amount found ± SD*	Recovery (%)	RSD (%)	Amount added ($\mu g\ mL^{-1}$)	Amount found ± SD*	Recovery (%)	RSD (%)
R2	0.100	0.105 ± 0.002	104.10	1.92	0.0100	0.0101 ± 0.0002	100.53	1.76
	1.004	0.990 ± 0.005	98.56	0.55	0.1004	0.1006 ± 0.0049	100.21	4.90
	10.040	9.999 ± 0.050	99.60	0.50	1.0040	0.9616 ± 0.0355	95.78	3.69
R4	0.102	0.104 ± 0.001	101.49	0.71	0.0102	0.0103 ± 0.0005	101.40	4.85
	1.020	1.034 ± 0.002	101.32	0.21	0.1020	0.1058 ± 0.0035	103.75	3.34
	10.200	10.128 ± 0.057	99.29	0.56	1.0200	0.9969 ± 0.0533	97.74	5.35
R3	0.104	0.109 ± 0.001	104.92	0.96	0.0104	0.0101 ± 0.0004	97.33	3.87
	1.036	1.046 ± 0.001	100.96	0.13	0.1036	0.1057 ± 0.0042	102.07	3.95
	10.360	10.457 ± 0.056	100.93	0.54	1.0360	1.0071 ± 0.0224	97.21	2.22
Torasemide	69.650	70.570 ± 0.160	101.32	0.23	0.6965	0.6781 ± 0.0263	97.36	3.88
	99.500	101.663 ± 0.161	102.17	0.16	0.9950	0.9589 ± 0.0202	96.37	2.11
	129.350	129.915 ± 0.727	100.44	0.56	1.2935	1.2684 ± 0.0548	98.06	4.32
R6	0.103	0.106 ± 0.002	102.33	1.92	0.0103	0.0106 ± 0.0003	102.48	3.05
	1.034	0.999 ± 0.001	96.57	0.12	0.1034	0.1057 ± 0.0035	102.25	3.28
	10.340	10.310 ± 0.055	99.71	0.53	1.0340	1.0155 ± 0.0564	98.21	5.56

* $n = 3$

added amount of analyte spiked into placebo mixture. On the other side, the precision (repeatability) was assessed as relative standard deviation (RSD) of a series of measurements. Accuracy and precision studies were performed at three different concentrations with three replicates covering the specified range. For the LC–UV analysis, the concentration levels were 70, 100 and 130 $\mu g\ mL^{-1}$ for torasemide and 0.1, 1.0 and 10 $\mu g\ mL^{-1}$ for impurities. For the LC–MS analysis, the concentration levels were 0.7, 1.0 and 1.3 $\mu g\ mL^{-1}$ for torasemide and 0.01, 0.1 and 1.0 $\mu g\ mL^{-1}$ for impurities. The results from examination of accuracy and precision are presented in Table VII. The obtained recovery values indicated good accuracy of both methods. Taking the RSD for each concentration into consideration, both LC–UV and LC–MS methods showed satisfactory precision.

The minimum level at which the analyte can be reliably detected (LOD) and quantified (LOQ) were determined experimentally for both methods. LOD and LOQ were defined as the amounts for which the signal-to-noise ratios were 3:1 and 10:1, respectively (20). These data are presented in Table VI.

All obtained validation parameters fulfilled the requirements according to ICH regulations. Comparing the methods, LC–UV shows better precision, whereas the LC–MS method is 50–100-fold more sensitive. After validation, the applicability of the method for determination of torasemide and impurities R2, R3, R4 and R6 was examined by analyzing commercially available Diuver tablets. The torasemide content was 96.3% determined by LC–UV and 0.15% for impurity R2. The impurities R3, R4 and R6 were not detected in LC–UV analysis. In LC–MS analysis, the content of torasemide was 96.8% and the content of impurity R2 was 0.16%. The impurities R3 and R6 were not detected, whereas impurity R4 was found below LOQ in LC–MS analysis. The results obtained by quantitative analysis met acceptance criteria. The low RSD value (less than 2%) for all determinations ($n = 3$) confirm the suitability of both methods, LC–UV and LC–MS, for the routine determination of torasemide and its impurities in dosage form. Chromatogram of sample solution of torasemide tablets obtained using LC–UV detection is displayed in Figure 5C.

Conclusion

LC–UV and LC–MS methods for simultaneous determination of torasemide and its impurities have been developed and validated. The experimental design is shown to be useful tool for evaluation of chromatographic behavior and optimal chromatographic conditions of the investigated substances. For both methods, the calibration curves showed high linearity over a wide concentration range and all requirements for method accuracy and precision are fulfilled. Compared to LC–UV analysis, LC–MS analysis added specificity that improved sensitivity (lower LOD and LOQ values were obtained) and increased confidence in the results of qualitative analysis of analytes. The proposed LC–MS method could be very valuable in further investigation during forced degradation studies. Considering validation parameters, both methods are sensitive, specific and reproducible enough to be applied in the quality control of torasemide and its impurities in active pharmaceutical ingredients and pharmaceutical dosage forms.

Acknowledgments

This research was supported by Ministry of Education and Science of the Republic of Serbia as the part of the project No. 172033.

References

1. Sweetman, S.; Martindale, the complete drug reference 36. E-Publishing; Pharmaceutical Press, London, (2009).
2. El-Sheikh, A.A.K., Masereeuw, R., Russel, F.G.M.; Mechanisms of renal anionic drug transport; *European Journal of Phamacology*; (2008); 585: 245–255.
3. Hardman, J.G., Limbird, L.E., Gilman, A.G.; The pharmacological basis oftherapeutics, 10th ed. Goodman & Gilman's, McGraw-Hill, New York, NY, (2001), pp. 757.
4. PDR Staff; Physicians' desk reference, 62nd ed. Thomson Healthcare Inc., Montvale, NJ, (2007).
5. Ferrara, N., Leosco, D., del Prete, M., Lombardi, L., Landino, P., Abete, P., *et al.*; Torasemide versus furosemide in patients with congestive heart failure: a double masked, randomized study; *Current Therapeutic Research*, (1997); 58: 291–299.

6. ICH Harmonised Tripartite Guideline. Impurities in new drug substances, Q3A (R2), Current Step 4 Version; (2006).
7. ICH Harmonised Tripartite Guideline. Impurities in new drug products, Q3B (R2), Current Step 4 Version; (2006).
8. Kondo, N., Kimura, M., Yamamoto, M., Hashimoto, H., Kawamata, K., Kawano, K., *et al.*; Chemical structure and physico-chemical properties of torasemide; *Iyakuhin Kenkyu*, (1994); 25: 734–749.
9. Liu, K., Lee, Y., Ryu, J., Lee, D., Kang, W., Lee, S.S., *et al.*; Simple and sensitive assay of torasemide in human plasma by high–performance liquid chromatography using a monolithic silica column; *Chromatographia*, (2004); 60: 639–643.
10. Engelhardt, S., Meineke, I., Brockmöller, J.; Improved solid–phase extraction and HPLC measurement of torasemide and its important metabolites; *Journal of Chromatography B*, (2006); 831: 31–35.
11. Barroso, M.B., Alonso, R.M., Jimenez, R.M.; Simultaneous determination of torasemide and its major metabolite M5 in human urine by high-performance liquid chromatography–electrochemical detection; *Journal of Chromatographic Science*, (2001); 39: 491–496.
12. Barroso, M.B., Meiring, H.D., de Jong, A., Alonso, R.M., Jimenez, R.M.; Gas chromatographic–mass spectrometric analysis of the loop diuretic torasemide in human urine; *Journal of Chromatography B*, (1997); 690: 105–113.
13. Akesolo, U., Gonzalez, L., Jimenez, R.M., Alonso, R.M.; Multivariate optimisation of a cyclodextrin–assisted–capillary zone electrophoretic method for the separation of torasemide and its metabolites; *Journal of Chromatography A*, (2003); 990: 271–279.
14. Deventer, K., Pozzo, O.J., van Eenoo, P., Delbeke, F.T.; Qualitative detection of diuretics and acidic metabolites of other doping agents in human urine by high-performance liquid chromatography–tandem mass spectrometry; *Journal of Chromatography A*, (2009); 1216: 5819–5827.
15. Qin, Y., Wang, X.B., Wang, C., Zhao, M., Wu, M.T., Xu, Y.X., *et al.*; Application of high-performance liquid chromatography–mass spectrometry to detection of diuretics in human urine; *Journal of Chromatography B*, (2003); 794: 193–203.
16. Goebel, C., Trout, G.J., Kazlauskas, R.; Rapid screening method for diuretics in doping control using automated solid phase extraction and liquid chromatography–electrospray tandem mass spectrometry; *Analytica Chimica Acta*, (2004); 502: 65–74.
17. Marchi, I., Rudaz, S., Veuthey, J.; Sample preparation development and matrix effects evaluation for multianalyte determination in urine; *Journal of Pharmaceutical and Biomedical Analysis*, (2009); 49: 459–467.
18. Riekkola, M., Jumppanen, J.H.; Capillary electrophoresis of diuretics; *Journal of Chromatography A*, (1996); 735: 151–164.
19. Ardrey, R.E.; Liquid chromatography–mass spectrometry, an introduction; John Wiley & Sons, West Sussex, England, (2003).
20. ICH Harmonised Tripartite Guideline. Validation of analytical procedures, text and methodology, Q2 (R1), Current Step 4 Version; (2005).
21. Dejaegher, B., van der Heyden, Y.; The use of experimental design in separation science; *Acta Chromatographia*, (2009); 21: 161–201.
22. Mendez, A., Bosch, E., Roses, M., Neue, U.D.; Comparison of the acidity of residual silanol groups in several liquid chromatograph columns; *Journal of Chromatography A*, (2003); 986: 33–44.
23. Preu, M., Guyot, D., Petz, M.; Development of a gas chromatography-mass spectrometry method for the analysis of aminoglycoside antibiotics using experimental design for the optimisation of the derivatisation reactions; *Journal of Chromatography A*, (1998); 818: 95–108.
24. Martendal, E., Budziak, D., Carasek, E.; Application of fractional factorial experimental and Box-Behnken designs for optimization of single-drop microextraction of 2,4,6-trichloroanisole and 2,4,6-tribromoanisole from wine samples; *Journal of Chromatography A*, (2007); 1148: 131–136.
25. Ferreira, S.L.C., Bruns, R.E., Paranhos da Silva, E.G., Lopes dos Santos, W.N., Quintella, C.M., David, J.M., *et al.*; Statistical designs and response surface techniques for the optimization of chromatographic systems; *Journal of Chromatography A*, (2007); 1158: 2–14.
26. Mason, R.L., Gunst, R.F., Hess, J.L.; Statistical design and analysis of experiments, 2nd ed. John Wiley & Sons, New York, NY, (2003), pp. 568.
27. European Pharmacopoeia. Cedex; 6th ed., Council of Europe, Strasbourg (2008).
28. Deventer, K., van Eenoo, P., Delbeke, F.T.; Simultaneous determination of beta-blocking agents and diuretics in doping analysis by liquid chromatography/mass spectrometry with scan to scan polarity switching; *Rapid Communications in Mass Spectrometry*, (2005); 19: 90–98.
29. Deventer, K., Delbeke, F.T., Roels, K., van Eenoo, P.; Screening for 18 diuretics and probenecid in doping analysis by liquid chromatography–tandem mass spectrometry; *Biomedical Chromatography*, (2002); 16: 529–535.
30. Thieme, D., Grosse, J., Lang, R., Mueller, R.K., Wahl, A.; Screening, confirmation and quantitation of diuretics in urine for doping control analysis by high-performance liquid chromatography–atmospheric pressure ionisation tandem mass spectrometry; *Journal of Chromatography B*, (2001); 757: 49–57.